Meteorology and elephant infrasound at Etosha National Park, Namibia

David Larom and Michael Garstang
Department of Environmental Sciences, University of Virginia, Charlottesville, Virginia 22903

Malan Lindeque
Ministry of Environment and Tourism, Directorate of Resource Management, Private Bag 13306, Windhoek, Namibia

Richard Raspet
National Center for Physical Acoustics, University of Mississippi, University, Mississippi 38677

Mark Zunckel, Yvonne Hong, Kevin Brassel, and Sean O'Beirne
Atmospheric Impacts Management, CSIR, Ematek, P.O. Box 395, Pretoria 0001, Republic of South Africa

Frank Sokolic
Department of Geographical and Environmental Sciences, University of Natal, Durban 4001, Republic of South Africa

(Received 22 November 1995; accepted for publication 6 October 1996)

Measured vertical profiles of temperature and wind are used to model infrasound propagation over a representative high savanna habitat typically occupied by the African elephant, *Loxodonta africana*, to predict calling distance and area as a function of the meteorological variables. The profiles were measured up to 300 m above the surface by tethered balloon-borne instruments in Etosha National Park, Namibia, during the late dry season. Continuous local surface layer measurements of wind and temperature at 5 and 10 m provide the context for interpreting the boundary layer profiles. The fast field program (FFP) was used to predict the directionally dependent attenuation of a 15-Hz signal under these measured atmospheric conditions. The attenuation curves are used to estimate elephant infrasonic calling range and calling area. Directionality and calling range are shown to be controlled by the diurnal cycle in wind (shear) and temperature. Low-level nocturnal radiative temperature inversions and low surface wind speeds make the early evening the optimum time for the transmission of low-frequency sound at Etosha, with range at a maximum and directionality at a minimum. As the night progresses, a nocturnal low-level wind maximum (jet) forms, reducing upwind range and calling area. The estimated calling area drops rapidly after sunrise with the destruction of the inversion. Daytime calling areas are usually less than 50 km^2, while early evening calling areas frequently exceed 200 km^2 and are much less directional. This marked diurnal cycle will be present in any dry savanna climate, with variations due to local topography and climate. Calling range and low-frequency sound propagation cannot be effectively understood without knowledge of meteorological controls. [S0001-4966(97)01803-1]

PACS numbers: 43.80.Ev, 43.80.Jz, 43.80.Ka, 43.64.Tk [FD]

INTRODUCTION

The use of low-frequency sound by terrestrial mammals has been most clearly documented for the African (*Loxodonta africana*) and the Asian elephants (*Elephas maximus*).[1–3] *L. africana* employs infrasonic calls with fundamental frequencies of 14–35 Hz for several vital purposes, including reproduction and herd assemblage. Most of the acoustic energy of these calls is concentrated at the fundamental frequency. To date, Langbauer *et al.*[4] have performed the only field experiment aimed at determining the range of the elephant's infrasonic calls. They demonstrated that elephants responded to the playback of recorded infrasonic calls from distances of 1.2 and 2 km. Playback stimuli, because of limitations of the loudspeakers used, were broadcast at only half the amplitude (−6 dB) of the known actual strongest elephant calls. In the simplest approximation, the 6-dB reduction corresponds to a halving of the effective broadcast distance, suggesting that the strongest elephant calls were in fact audible to conspecifics at least 4 km away. This extrapolation, however, assumes that the playback sound will propagate with essentially no excess attenuation or enhancement due to surface effects or meteorological conditions.

Martin[5] observed apparent coordinated movements of herds in Zimbabwe, and hypothesized that elephants can communicate over distances up to 5 km under conditions where visual and olfactory signals are not possible. Garstang *et al.*[6] suggested that, under optimum atmospheric conditions, elephants could communicate over ranges in excess of 10 km. Calculated acoustic enhancement was greatest for the lowest of two frequencies modeled (15 and 30 Hz) and occurred when inversions of temperature of more than 20-m

height were present under calm or low wind speed conditions. The combination of a near surface inversion with low wind speeds occurs most frequently in the early evening over the elevated African savannas. Such evenings occur more often in the dry season or during dry periods. Garstang *et al.*[6] thus showed that there are pronounced diurnal (and perhaps larger scale) fluctuations in the range over which low-frequency sound is transmitted.

The report of Garstang *et al.*[6] was, however, based upon idealized atmospheric temperature profiles and examined neither the detailed time variations of actual observed profiles nor the effects of wind velocity or wind shear. The present study uses measured vertical profiles of temperature and wind to model infrasound propagation over a representative high savanna habitat at the end of the southern African dry season. These observations were taken by tethered balloon at Okaukuejo (19° S latitude, 16° E longitude) in the Etosha National Park, Namibia, as part of the 45-day Southern African Fire–Atmosphere Research Initiative (SAFARI) experiment (M. O. Andreae, personal communication). The profiles are used as input to the fast field program (FFP) to predict the acoustic attenuation. The calling area of a 15-Hz signal is estimated as a function of specified meteorological controls. The results strengthen Garstang *et al.*'s[6] prediction that the early evening is an optimum time for long distance communication, but show that range, direction, and calling area are strongly influenced by the diurnal evolution of the changes of near-surface thermal and kinematic structure of the atmosphere. The present paper delineates the complexity of this evolution and of the consequent acoustic fields.

I. THE AIR NEAR THE GROUND

A. Large-scale considerations

The Etosha National Park lies on the western escarpment of southern Africa at a mean elevation of about 1100 m, immediately east of the Skeleton Coast and northeast and northwest of the Namib and Kalahari deserts, respectively. The weather and climate of the region are dominated by the subtropical anticyclone. The large-scale atmospheric subsidence typical of anticyclonic circulations is amplified by the Benguela current, which flows northwards from Antarctica, and by upwelling of cold bottom water. Both factors create extremely cold sea surface temperatures of 14 °C–15 °C along the west coast of southern Africa. This cools the air above, suppressing atmospheric convection and vertical moisture transport. Humidity and cloudiness are therefore suppressed. Mean annual rainfall at Okaukuejo is about 360 mm, with pronounced wet (November–April) and dry seasons (May–October). The SAFARI experiment took place during the end of the 1992 dry season, as a prolonged and severe drought was ending; 3.2 mm of rain fell on 28 September. Light rain was measured on 10 October, and a trace of precipitation was measured on 9 and 11 October.

Precipitation in this and similar dry African savanna climates is typically in the form of brief thundershowers. The skies clear rapidly after these convective storms. Even during the rainy season, days with continuous cloud cover or high humidity are rare. High solar insolation during the day and rapid radiative cooling at night are thus the norm for most of the year. Temperatures at the soil–air interface often exceed 40 °C at solar noon. As the day progresses and the sun lowers, the ground begins to cool. Atmospheric water vapor is an important greenhouse gas buffering the nighttime cooling by absorption and emission of long wave radiation. Since humidity at Etosha is low, radiative cooling is rapid and air–surface interface temperatures often fall below 15 °C before sunrise. This diurnal oscillation in surface temperatures gives rise to very pronounced nocturnal temperature inversions; temperatures may rise by as much as 10 °C from the surface to 50-m elevation. Conversely, daytime surface temperatures are high but drop rapidly with height.

Nocturnal inversions form prior to sunset and persist until just after dawn under these conditions. The surface layer is frictionally decoupled from the deeper atmosphere with calm or near calm winds and little or no turbulence. Winds above the surface layer, however, accelerate in response to reduced surface friction and large scale pressure gradients. Continued nocturnal cooling causes the cold surface air to accelerate downslope, even if the slopes are very mild. The combined accelerations result in strong wind shear and change in wind direction across the boundary between the cold surface and the warmer overlying air. Later in the evening, mechanical turbulence induced by this wind shear mixes the air between the layers, reducing and elevating the early evening inversion.

B. Atmospheric surface layer

1. Solar and terrestrial radiation and surface temperatures

Global radiation measurements taken over 40 days of the 45-day field experiment show that close to 50% of the days were clear, 25% partly cloudy, and 25% cloudy. On the clear days the net outgoing long wave radiation (long wave losses from the surface+long wave radiation received from the atmosphere) exceeds the incoming short wave radiation (global short wave) (1-albedo) from shortly before sunset until shortly after sunrise. In response to the radiative balance, the atmosphere near the surface cools rapidly after 1600 Local Solar Time [Local Solar Time (LST) is used because of the solar control of radiative cooling and heating of the surface], commonly displaying a cooling rate of about −1.3 °C/h, as shown in Fig. 1. Air temperatures at 10 m above the ground reach maximum temperatures on clear days of 30 °C around 1400 LST. Cooling over the next 14 h produces a drop of over 18 °C, yielding a near-surface air temperature below 12 °C. After sunrise soil and air temperatures rise rapidly to their daytime maxima.

2. Surface wind

The pronounced diurnal cycle in temperature is reflected in measurements of wind speed and direction. Figure 2 shows a typical diurnal sequence of wind speed and direction. Fifteen days of the experiment show a similar structure. High daytime wind speeds and a northeasterly wind direction typify the dominant circulation associated with the southern African continental anticyclone (anticyclones rotate counter-

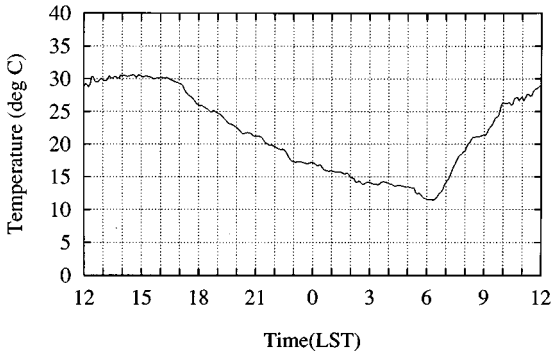

FIG. 1. Air temperature at Okaukuejo, Etosha National Park, Namibia at 10 m, 22–23 September 1992. *X* axis: Local Standard Time (LST). *Y* axis: Air temperature in degrees centigrade.

clockwise in the southern hemisphere). At night, wind speeds decrease greatly, due to the decoupling of the stable nocturnal atmospheric boundary layer from the free atmosphere above. The light southerly winds are due to drainage flow from low mountains to the south.

Mean daily (24 h) wind speeds are low, averaging 2.5 and 3.5 m s^{-1}, respectively, at 5 and 10 m. Mean hourly wind speeds show a pronounced semi-diurnal signature, with the lowest wind speeds occurring an hour after sunrise and sunset. The strongest winds (>4 m/s) occur over a 6-h period centered on solar noon. The greatest frequency of calm and winds between 0 and 1 m/s occurs between the hours of 1900

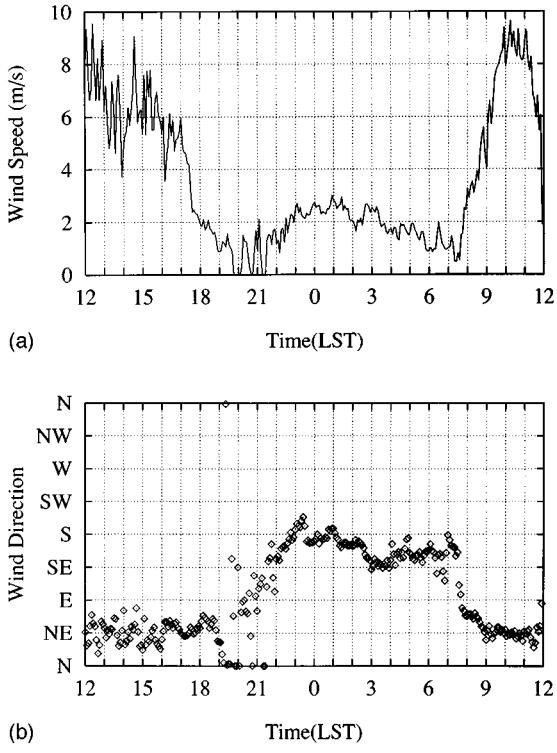

FIG. 2. (a) Wind speed at Okaukuejo, Etosha National Park, Namibia, at 10 m, 17–18 September 1992. *X* axis: Local Standard Time (LST). *Y* axis: Wind speed in m/s. (b) Wind direction at Okaukuejo, Etosha National Park, Namibia, at 10 m, 17–18 September 1992. *X* axis as for (a). *Y* axis: Wind direction (direction from which wind is coming). Letters (N, NE, etc.) depict wind direction with respect to true north.

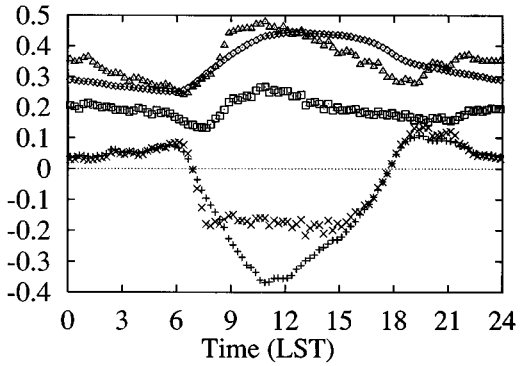

FIG. 3. Diurnal march of the average values of extrapolated surface temperature, T_0 (◇:°C*10^{-2}), temperature gradient dT/dz (+: °C/m), wind speed U at 10 m (△: m s^{-1}*10^{-1}), wind shear dU/dz (□: s^{-1}) and gradient Richardson number R_i (*x*: dimensionless). *X* axis: Local Standard Time (LST). *Y* axis: Value of the above-mentioned variables in the indicated units.

and 2100 at both 5 m and 10 m above the ground, with a secondary peak at sunrise. Five minute average wind speeds of 2 m/s or less occur about 40% of the time at 5 m and at about half this frequency at 10 m.

3. Temperature, wind gradients, and stability

Figure 3 shows the hourly average values of the extrapolated surface temperature (T_0), 10-m wind speed (U), wind shear (dU/dz), temperature gradient (dT/dz), and the gradient Richardson number (R_i). Here T_0, dU/dz, dT/dz, and R_i are calculated from the continuous tower measurements at 5 and 10 m. All of the variables show a response to daytime heating and nighttime cooling. The temperature gradient reaches a maximum shortly after sunset (1800 LST), decreases through the night, and rises to a secondary maximum just before sunrise (0600 LST). An opposite trend is found in the shear of the horizontal wind (dU/dz). Lowest shears are seen just after sunrise and sunset.

The effects of temperature lapse rates and wind shear are combined in the gradient Richardson number:

$$R_i = \frac{g}{\theta_0} \frac{d\theta/dz}{|dU/dz|^2},$$

where $\theta_0 = T_0(1000/890)^{0.286}$ is the surface potential temperature, and $d\theta/dz = dT/dz + 0.0098$ °C/m is the gradient of the potential temperature. Here, R_i is an index of atmospheric stability ($R_i > 0$ for a stable atmosphere, $R_i < 0$ for an unstable atmosphere). Since low-frequency sound transmission is optimized under stable atmospheric conditions with a positive temperature gradient and little or no wind shear, R_i may be a useful proxy for calling range or calling area.[7]

The diurnal progression of R_i in Fig. 3 indicates that conditions are unstable during the day but rapidly rise to maximum stability shortly after sunset. Stability follows a similar path to the temperature lapse, decreasing but remaining stable through the night, and rising to a secondary maximum before sunrise. Conditions quickly become unstable after sunrise.

TABLE I. Date, start time, and end time of tethersonde runs and number of soundings performed during SAFARI-92 in Okaukuejo, Namibia.[8]

Date	Start	End	Number of soundings
–09-14-92	0615	0900	4
–09-15-92	0630	0800	3
–09-16-92	0615	1000	5
09-16-92–09-17-92	1800	0900	8
09-17-92–09-18-92	1730	0900	8
09-18-92–09-19-92	1800	1000	8
09-19-92–09-20-92	1715	0900	11
09-20-92–	1800		1
09-21-92–09-22-92	1800	0615	3
09-22-92–09-23-92	1700	0900	5
09-23-92–09-24-92	1700	1000	11
09-25-92–09-26-92	1700	0900	11
09-26-92–	1715		1
09-27-92	1745	1900	2
09-28-92–09-29-92	1700	0700	8
09-30-92–10-01-92	1700	0815	11
10-01-92–10-02-92	1715	0900	8
10-02-92–	1700	1800	2
10-03-92	1900	2000	2
10-04-92–	1815		1
Total number of soundings			113

C. Atmospheric boundary layer

Under nonprecipitating conditions the atmospheric boundary layer may be defined as that part of the atmosphere above the surface layer in which the effects of the surface, such as surface friction and surface heating or cooling, are clearly discernible. The free atmosphere lies above the atmospheric boundary layer. The atmospheric boundary layer responds to surface heating, growing to a maximum height over land of 1200–1500 m above the surface soon after midday. Vertical profiles of temperature, humidity, pressure, and horizontal wind speed and direction were taken through the surface and boundary layers, by means of a tethered balloon system described by Zunckel *et al.*[8] A rate of ascent of the tethered balloon instrument package of about 1 m/s provides high vertical resolution of the measured fields. Table I shows the number of soundings and time intervals during the day for 113 soundings taken during the field experiment. Of the 113 soundings, all but 8 reached a height of greater than 100 m, and 65 exceeded 300 m. Soundings were made through the night on 12 occasions. Table II summarizes observed inversion strength and height just before and following sunset and sunrise. Adiabatic ($dT/dz=-9.8$ °C/km) to superadiabatic ($dT/dz<-9.8$ °C/km) conditions prevailed during the day, in response to strong convective mixing above the hot surface. On clear evenings when radiative cooling was greatest, near-surface inversions formed and decayed rapidly. Inversion conditions, in which cold dense air close to the ground is overlain by a warmer, less dense layer of air, effectively decouple the deeper atmosphere from the surface layer. Air that was frictionally slowed by the ground and by vegetation is now separated from the surface by a layer of cold air. This frictional decoupling, combined with the downslope flow of cold air and inertial accelerations from the Coriolis force, produces a low-level nocturnal jet.[9–12]

Figure 4 shows the evolution of the low-level thermal and wind speed fields during a representative night (19–20 September 1992). The data are given as contour plots with time represented on the x axis and height above ground on the y axis. The contour plots were constructed from interpolation of tethered balloon soundings taken at 1610, 1702, 1800, 2000, 2200, 0020, 0410, 0500, 0600, and 0802 LST. After 1700 LST, wind speeds decrease to less than 2 m s^{-1} throughout the boundary layer, and a low-level temperature inversion forms. After 2200 the nocturnal jet begins to form; by 2300 it is well established. During this time period, strong

TABLE II. Characteristics of tethersonde temperature profiles measured at various times of day during SAFARI-92 in Okaukuejo, Namibia. Asterisks (*) indicate that inversion strength and height may have been greater; balloon was unable to ascend further. Inversion strength≡maximum temperature in sounding −1.5 m temperature. Inversion height≡height of highest temperature reading (after Zunckel *et al.*[8]).

	Average inversion strength (°C/km)	Inversion strength range (°C)	Inversion height (m)	Inversion height range (m)
1600	No inversion			
1700	0.47	0.05–1.67	~20	
1800	2.13	0.38–3.88	59	33–139
2000	4.83	0.77–9.35	96	80–137
0500	4.49*	0.68–10.85*	102	30–240
0600	5.93	2.16–13.05	128	63–227
0700	3.22	1.34–7.52*	130	30–485
0800	2.56	0.57–5.70	131	30–480

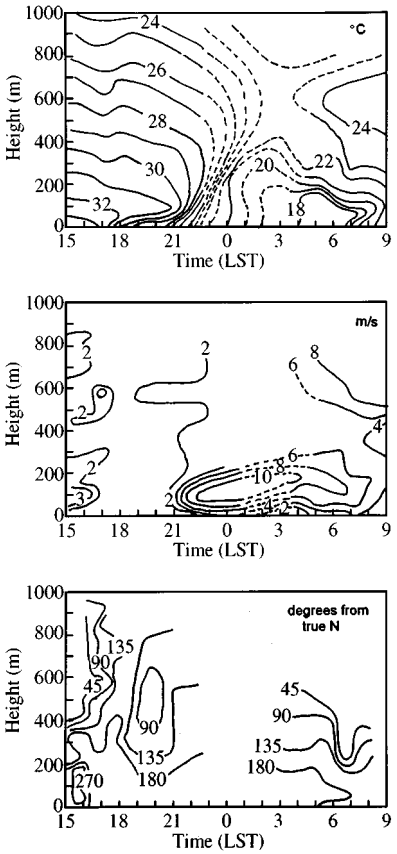

FIG. 4. Contours of temperature in °C (top), wind speed in m/s (middle) and wind direction in degrees from true north (bottom), for 19–20 September 1992. Constructed from the tethersonde profiles of Fig. 6. X axis: Local Standard Time. Y axis: Height above ground in m (after Zunckel *et al.*[8]).

low-level wind shear generated by the jet mixes cold low-level air with warmer air above, lessening the temperature gradient and raising the height of the inversion. From 0000 until the demise of the jet after sunrise, vigorous mixing produced by the jet, together with radiative cooling of the ground, induces a uniform cooling rate of approximately 1 °C h^{-1} in the lowest 200 m. Above this height the unmixed warmer air remains, forming an elevated inversion which persists 2 h or more after sunrise.

This temporal evolution of the thermal and velocity fields in the atmospheric boundary layer is common and widespread over the savannas of southern Africa. Since the low-level temperature gradient and wind shear are the main atmospheric controls on low-frequency sound propagation,[6] it is to be expected that there will be a strong diurnal cycle in the range and directionality of calls made by animals employing infrasound for long-distance communication. This hypothesis is explored in the following section.

II. OPTIMUM CONDITIONS FOR LOW-FREQUENCY SOUND TRANSMISSION

There are numerous computational and analytic solutions which predict atmospheric sound propagation based upon the vertical profiles of temperature and wind velocity. Most of these, however, assume that sound travels in rays.[13] This assumption applies only for high-frequency sound propagation in the atmosphere and is unsuitable for infrasonic frequencies. The present study uses a numerical solution of the acoustic wave equation to predict attenuation in a thermally and velocity stratified medium above an impedance surface. The solution is a fast field program or FFP, first developed for underwater sound propagation and modified for atmospheric propagation by Raspet *et al.*[14] and Lee *et al.*[15] A detailed description of this modified FFP is given by Franke and Swenson,[16] and its employment as a tool to predict the attenuation of elephant infrasonic calls is described by Garstang *et al.*[6] In brief, the assumption of a radially symmetric velocity field enables wind shear to be incorporated into a cylindrically symmetric, Helmholtz equation,

$$\frac{\partial^2 p}{\partial r^2}+\frac{1}{r}\frac{\partial p}{\partial r}+\frac{\partial^2 p}{\partial z^2}=\frac{2}{r}\,\delta(r)\,\delta(z-z_s),$$

where p=pressure, r=horizontal distance from the source, z_s=source height, and z=receiver height. The solution employs a Hankel transform to reduce the Helmholtz equation to a form of Bessel's equation in the transformed domain. The transformed equation is solved by analogy to the ''telegrapher's equations,'' with branch points and poles on the real axis avoided by the introduction of an ''artificial attenuation.'' The integral in the wave number space is approximated by a sum, and a single fast Fourier transform (FFT) yields $p(r,z)$.

Garstang *et al.*,[6] in a study of low-frequency sound transmission, found that the presence of atmospheric inversions of temperature enhanced transmission, while adiabatic and superadiabatic lapse rates significantly attenuated the signal. These results were, however, based upon simplified inversion structures, and the atmosphere was assumed to be at rest. The characterization of acoustic fields in an atmosphere in motion, using measured temperature and wind profiles, is considerably more complex.

In an atmosphere in motion, the direction of greatest range of low-frequency sound transmission may not be directly downwind. High positive wind shear causes the outwardly propagating acoustic waves to interact strongly with the ground; this absorbs energy and degrades the signal. A more intuitive explanation, though not strictly accurate for low frequencies, may be made by thinking of sound in terms of rays. Moderate wind shear will cause sound to bend downward, bringing extra rays to the receiver. However, strong wind shear causes multiple-bounce rays. Since each bounce absorbs energy, propagation directly downwind is not optimum. Maximum calling range can thus occur at an angle (less than 90°) from directly downwind. Further complicating this argument is the fact that, for a real sounding in which backing or veering (decrease or increase of wind direction with height) are present, ''downwind'' is an abstraction rather than a physical reality. Variation of wind speed and direction with height will produce asymmetric fluctuations in range and direction of propagation of the sound waves.

In the real atmosphere, particularly under the conditions studied in the Etosha National Park at the end of the dry season, marked changes in the thermal and velocity fields are seen over the diurnal cycle (Figs. 3 and 4). A numerical solution to the acoustic wave equation in the form of the fast field program (FFP), also applied and described in detail by Garstang *et al.*,[6] is used to calculate the attenuation of 15-Hz sound as a function of the vertical profiles of temperature and of the component of the wind speed in the direction of propagation. These directional predictions of acoustic fields are then used to find the optimal times to predict the range, and to characterize the temporal evolution and variability of elephant calling.

A. Nocturnal enhancement

The atmosphere will have no influence on surface-to-surface sound propagation above a certain height. A conservative minimum height of 300 m was chosen.[17] Based on this consideration, 65 of the 113 tethered balloon profiles were used as input for the FFP. The other profiles did not reach a height of 300 m. Decibel attenuation contours for each profile were obtained by calculating the directionally dependent attenuation in 24 increments of 15°. A separate FFP run was required for each direction, necessitating 24 runs for each profile. Attenuation contours were plotted for a frequency of 15 Hz. The complex impedance was calculated by FFP, using Attenborough's four-parameter model[18] and an estimated flow resistivity of 500 000 mks rayls/m. Calling ranges for higher frequencies or softer ground may be expected to be smaller.

Human hearing compared to that of elephants is very poor at low frequencies. Hearing thresholds are approximately 93 dB (all dB references are re 20 μPa rms at 1 m) at 15 Hz and 70 dB at 30 Hz. Elephant hearing at these same frequencies is markedly better.[19] A study by Heffner and

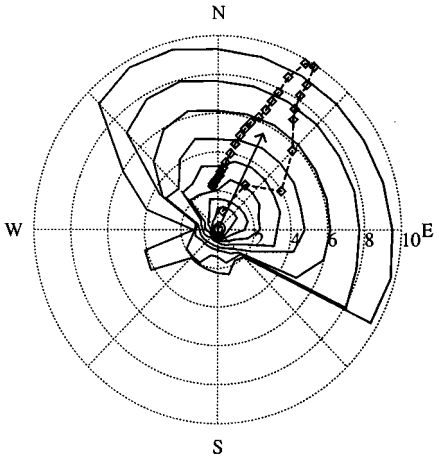

FIG. 5. Attenuation contours (closed solid lines) and wind hodograph (--□--) for 2200 LST, 19 September 1992. Contours are plotted in −3-dB increments from the innermost (−40 dB) to the outermost (−67 dB). Points on the wind hodograph give the terminus of the velocity vector in 25-m height increments from ground level to 300 m. Arrow indicates average wind in the first 300 m above the ground. Numbers (2,4,6, etc.) indicate both the distance in km from the source (for the attenuation contours) and the wind speed in m/s (for the hodograph and average wind arrow). Letters (N,E,S,W) show direction of wind and of sound propagation, with respect to true north.

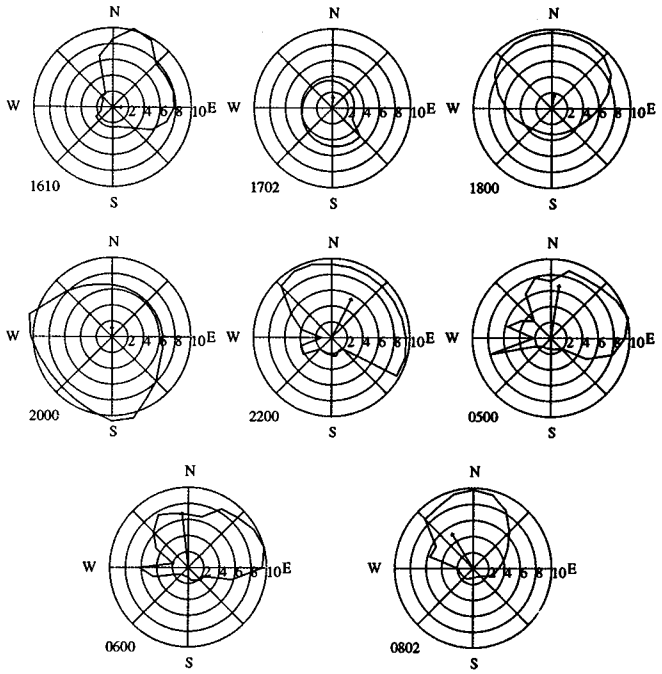

FIG. 6. The −67-dB attenuation contour predicted via FFP (irregular closed line depicting range in km) and mean wind in first 300 m (arrow: space in m s^{-1}) from tethered balloon soundings made on 19–20 September 1992 in Okaukuejo, Namibia. Time of sounding (LST) is given in lower left of each plot. Letters and numbers as in Fig. 5.

Heffner[20] gives the elephant hearing threshold at 16 Hz as 65 dB. This approximates to 68 dB at 15 Hz, rapidly improving to 43 dB at 30 Hz. However, these results are from one 7-year-old Indian elephant. The lowest reasonable threshold for a full grown African elephant was assumed to be 50 dB. Because the present study is primarily concerned with the diurnal variation in calling range and calling area, rather than the absolute magnitudes thereof, substitution of a greater or lesser value will not invalidate our conclusions.

The most intense elephant infrasonic signal reported in the literature is 117 dB.[3] With a sound level of 117 dB and a hearing threshold of 50 dB, an estimate of calling range is given by 117 dB+attenuation=50 dB. For the present study, the calling range is therefore defined as that range at which the attenuation is −67 dB. Figure 5 depicts a typical set of attenuation contours (for 2200 LST, 19 September 1992). The temperature and wind fields yielding these contours are given in Fig. 4. Contours are plotted in −3-dB increments from the innermost (−40 dB) to the outermost (−67 dB). The main features of Fig. 5 are present in many other sounding contours. There is a marked asymmetry, with degraded calling range ''upwind'' and enhanced range ''downwind.'' The sharp drop in range from NW to W and from E to SE is likely due to a combination of strong wind shear and change in wind direction with height. It may also in part be an artifact of the authors' simplifying assumption that the calling range is defined by the first radius at which the attenuation drops below −67 dB. In some profiles, the attenuation will drop below −67 dB and then rise above −67 dB at a greater distance from the source. Examination of these regions of ''anomalous propagation''[21] is deferred to a future study.

Figure 5 shows that the range of propagation downwind from the source is roughly five times greater than the range upwind. The innermost contours are nearly circular, moving outwards the contours first become extended in the downwind direction and then broaden considerably in the crosswind direction. The shapes become increasingly jagged with higher attenuation. These irregularities of shape are largely due to the fluctuations in the measured wind and temperature fields. Since these fluctuations do not persist in time, the irregularities in the contours are not relevant; the general elliptical shape is the important factor. The range of maximum and minimum low-frequency sound propagation is not directly upwind or downwind, for reasons previously stated.

B. Case study of combined thermal and kinematic controls

Figure 6 depicts the temporal evolution of the −67-dB contours of a 15-Hz signal over the night of 19–20 September 1992. These are used as an estimate of elephant calling range and calling area. At 1610 LST, a nearly adiabatic temperature gradient of −9.0 °C/km is combined with winds of approximately 2 m s^{-1} (Fig. 4). The winds are westerly to 150 m and highly variable from 150–300 m. This yields a very directional contour; the calling range is less than 2 km in the ''upwind'' direction and 8–10 km ''downwind.'' The region of extended range (>6 km) is concentrated in the quadrant from north to east.

An hour later (Fig. 4), ground cooling has commenced and a 40-m-thick layer of 32 °C air underlies the adiabatic zone. Winds have shifted to southerly and lessened slightly with the commencement of drainage flow from the hills to the south, and the range is 3–5 km in all directions. At 1800 the wind is essentially the same, but a temperature inversion of 2.7 °C strength and height of 42 m has formed. This en-

hances the range to over 9 km ''downwind,'' but shortens it to 3 km ''upwind.'' Although the minimum and maximum ranges are similar to those given by the 1610 sounding, the area covered is greater due to the broader shape. The zone in which the range is greater than 6 km now extends of over 180 ° from E to N to W, as opposed to the 90° of the 1610 sounding. This broad zone of extended range is characteristic of nocturnal soundings.

By 2000 the wind speeds are below 2 m s^{-1}. Wind shear is nonexistent or very mild above 2 m. The inversion has grown to 3 °C strength and 64-m height. This is the optimum calling time; the range goes beyond 10 km in two lobes to the west and south, and everywhere exceeds 6 km. (This is a typical evening optimum: in the most pronounced cases, the range was 10 km or more in all directions.[7]) By 2200 the southerly jet has set in, and the inversion has grown to 6 °C strength and 221 m height. Strong wind shear has greatly decreased the upwind range; over the 180° from SE to N to NW, the range mostly exceeds 9 km, while from NW to S to SE it is seldom over 2 km.

Over the rest of the night, the inversion becomes elevated. The low-level wind shear remains strong and the winds stay southerly. No attenuation contours were plotted for 0200, 0410, or 0700 as the soundings did not reach to 300 m. From 0500 to 0600 (approximately sunrise) to 0802, the wind remains southerly to 150 m, but the 300 m winds back to northeasterly, their characteristic daytime direction. This directional shear may explain why the 0500 and 0600 range plots are highly asymmetric, lacking the rough bilateral symmetry of the previous contour fields. For these two soundings, the elevated inversion is underlain by a 100- to 150-m-thick layer of air of constant temperature or of a near-adiabatic temperature gradient. Again, this is due to mechanical mixing caused by the strong wind shear.

Around sunrise (0600), the jet begins to break up as the onset of ground heating causes thermal convection and mixing. The low-level wind shear becomes confined to the lowest 30 m as the velocity begins to be mixed more evenly through the boundary layer. This, combined with the lessening of the elevated inversion, gives rise to a more confined range contour. At 0802, the shape is similar to the 1610 contour; the zone of extended range is concentrated in a narrow lobe downwind and there is severe attenuation upwind.

C. Characterization of range plots

Due to the extreme directionality and irregularity of many of the range plots generated for the 65 soundings, it is difficult to characterize the degree of enhancement or attenuation of long-range infrasonic calling. The simplest indicator is the calling area A, the area enclosed within the −67-dB contour. Figure 7 depicts the temporal evolution of A. Each of the 65 usable soundings is represented by a single data point. Four temporal regions can be defined. The first region, 1600–1830 LST, is a time of rapid growth in A. The optimum calling time is 1830–2030, with A mostly exceeding 200 km^2. After 2030, A collapses rapidly to 150 km^2 and then shrinks slowly until sunrise at 0600. From then until 0900, A again diminishes rapidly to its daytime value, typically well below 50 km^2.

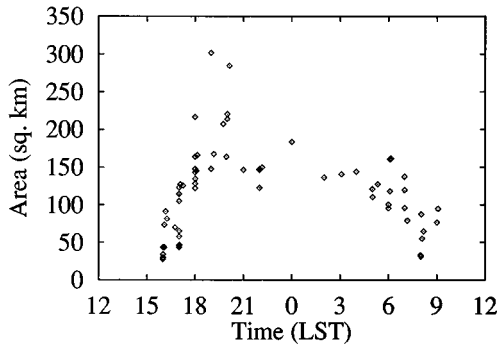

FIG. 7. Area (in square kilometers) covered by −67-dB attenuation contour as a function of time of day, for 65 tethered balloon soundings from 16 September to 4 October 1992. *X* axis: Local Standard Time. *Y* axis: Area in km^2.

Figure 7 shows that the case study of Fig. 6 is typical; although a nocturnal jet does not form every night, it forms with sufficient frequency that the trends in expansion and contraction of range in the case study are mirrored in Fig. 7. The following sequence of atmospheric controls and resultant calling range is hypothesized as a model of the diurnal cycle in calling area:

(i) 1600–1830: Rapid growth of A from 50 to 200 km^2 as winds die and the nocturnal inversion begins to form.
(ii) 1830–2030: Optimum time due to strong temperature gradients and low winds. A over 200 km^2.
(iii) After 2030: Collapse of A to below 150 km^2 due to onset of nocturnal jet.
(iv) 2030–0600: Slow diminishing of A from 150 to 125 km^2 as jet stabilizes and the inversion becomes elevated.
(v) 0600–0900: Second collapse to below 50 km^2 as solar radiation heats the ground, destroying the inversion and jet.
(vi) 0900–1600: Range below 50 km^2, perhaps much less.

III. CONCLUSIONS

The results of this paper are based on numerical predictions of 15-Hz signal propagation under measured atmospheric velocity and temperature profiles. Comparison with actual temporal patterns in elephant calling and reception is addressed in detail by Larom *et al.*[7] A study of 14 radio-collared and microphoned elephants in Zimbabwe[22] shows a late afternoon peak in loud, low-frequency elephant calls. This peak is caused by a pattern of late afternoon treks to water by elephants in this area, during the dry season. These treks require coordinated movements of each herd, necessitating calls. The timing is thought to be due to a combination of thirst at the end of a hot day, avoidance of predation of elephant calves by nocturnal predators, and transmission conditions considerably improved from midday. Further exploration of the role that atmospheric controls play in calling behavior will require a field study combining atmospheric measurements with simultaneous observation of elephants.

The vertical profiles of wind and temperature have strong and complex effects on ground-to-ground infrasound propagation at Etosha National Park. The formation of the

nocturnal temperature inversion in the early evening and its breakup with sunrise leads to a diurnal cycle in calling range, with a doubling or tripling of range after sunset. Optimal conditions occur one to two hours after sunset when winds are lowest and the inversion strongest. Shallow southerly gravity flow sets in later and is overlain by an easterly or southerly jet. This increase of wind during the night leads to a steady degradation and increased directionality of calling range as the night progresses. The increased wind shear also introduces mixing and weakens the temperature inversion, further degrading calling, until sunrise. However, the calling range at any time during the night is likely to be better than during the day, when adiabatic to superadiabatic temperature lapse rates combine with high ground-level winds, creating conditions highly detrimental to ground-to-ground low-frequency communication.

Infrasound propagation responds to the interactions between atmospheric thermal and velocity fields. In the dry, high-pressure-dominated atmosphere of the subtropics, thermal controls will exhibit a pronounced and predictable diurnal cycle. Wind velocity will exhibit a more complex cycle strongly influenced at night by topography. Even modest slopes of the ground surface will result in cold air drainage. During the early evening, stratification due to surface cooling will decouple the cold surface air from the warmer air above. Winds at the surface will die and calm or near calm conditions will prevail. Strong but shallow inversions with no wind will maximize low-frequency sound transmission during this part of the early evening. Both the range and the area over which low-frequency sound is transmitted will be maximized at this time. The calling area reaches a maximum and effects of directionality are at a minimum. Once drainage flow sets in, wind velocity becomes a factor and infrasound transmission becomes subject to the effects of both thermal stratification (now weaker) and wind shear. Both range and direction are affected and a marked directionality of propagation appears. Towards the end of the night, drainage flow may cease as cold air pools to capacity and the effects of air motion once again decline. Depending on local topography, this can lead to a second period of optimum low-frequency sound transmission conditions about dawn. Differences in relief and changing large-scale meteorological fields can disrupt the simple thermal response, which may be seen over a perfectly featureless and level plain. The thermal and velocity structure of the near surface atmosphere have a pronounced influence on low-frequency sound transmission at Okaukuejo. Any interpretation or application of low-frequency sound transmissions must take account of these temporal and spatial changes in calling range. No general conclusions can be drawn from observations of sound transmissions without concurrent attention being paid to the prevailing atmospheric conditions. Conversely, observations of low-frequency sound transmissions or communication can be effectively interpreted given only basic knowledge of atmospheric conditions and knowledge of the time of day of the infrasound observations. Similarly, any applied use of infrasound in the field should take account of atmospheric conditions which either enhance or interfere with the transmission of low-frequency sound.

ACKNOWLEDGMENTS

This paper draws upon the dissertation work of Mr. Larom at the University of Virginia. The field work for this study was carried out under the framework of the Southern African Fire–Atmosphere Research Initiative (SAFARI). The field work was supported by Grant ATM92-07924 and the analytical work by Grant ATM-9529315 from the National Science Foundation to the University of Virginia.

[1] K. Payne, W. R. Langbauer, Jr., and E. M. Thomas, ''Infrasonic calls of the Asian elephant (*Elephas maximus*),'' Behav. Ecol. Sociobiol. **18**, 297–301 (1986).

[2] W. R. Langbauer, Jr., K. B. Payne, K. B. R. A. Charif, and E. M. Thomas, ''Response of captive African elephants to playback of low-frequency calls,'' Can. J. Zool. **67**, 2604–2607 (1989).

[3] J. H. Poole, K. B. Payne, W. R. Langbauer, Jr., and C. J. Moss, ''The social contexts of some very low frequency calls of African elephants,'' Behav. Ecol. Sociobiol. **22**, 385–392 (1988).

[4] W. R. Langbauer, Jr., K. Payne, R. A. Charif, L. Rapaport, and F. Osborn, ''African elephants respond to distant playbacks of low-frequency conspecific calls,'' J. Exp. Biol. **157**, 35–46 (1991).

[5] R. B. Martin, ''Aspects of elephant social organization,'' Rhodesia Sci. News **12**, 184–187 (1978).

[6] M. Garstang, D. Larom, R. Raspet, and M. Lindeque, ''Atmospheric controls on elephant communication,'' J. Exp. Biol. **198**, 939–951 (1995).

[7] D. L. Larom, M. Garstang, K. Payne, R. Raspet, and M. Lindeque, ''The influence of surface atmospheric conditions on the range and area reached by animal vocalizations,'' J. Exp. Biol. (in press).

[8] M. Zunckel, Y. Hong, K. Brassel, and S. O'Beirne, ''Characteristics of the nocturnal boundary layer: Okaukuejo, Namibia during SAFARI-92,'' J. Geophys. Res. **101**, 23757–23766 (1996).

[9] A. K. Blackadar, ''Boundary layer wind maxima and their significance for the growth of nocturnal inversions,'' Bull. Am. Meteorol. Soc. **38**, 283–290 (1957).

[10] J. Holton, ''The diurnal boundary layer wind oscillation above sloping terrain,'' Tellus **19**, 199–205 (1967).

[11] S. Greco, S. Ulanski, M. Garstang, and S. Houston, ''Low-level nocturnal wind accelerations over the Central Amazon Basin,'' Bound. Layer Meteor. **58**, 91–115 (1992).

[12] M. Zunckel, G. Held, R. A. Preston-Whyte, and A. Joubert, ''Low-level wind maxima and the transport of pyrogenic products over southern Africa,'' J. Geophys. Res. **101**, 23745–23756 (1996).

[13] J. L. Spiesberger and K. M. Fristrup, ''Passive localization of calling animals and sensing of their acoustic environment using acoustic tomography,''Am. Nat. **135**, 107−153 (1990).

[14] R. Raspet, S. W. Lee, E. Kuester, D. C. Chang, W. F. Richards, R. Gilbert, and N. Bong, ''Fast-field program for a layered medium bounded by complex impedance surfaces,'' J. Acoust. Soc. Am. **77**, 345–352 (1985).

[15] S. W. Lee, N. Bong, W. F. Richards, and R. Raspet, ''Impedance formulation of the fast field program for acoustic wave propagation in the atmosphere,'' J. Acoust. Soc. Am. **79**, 628–634 (1986).

[16] S. J. Franke and G. W. Swenson, ''A brief tutorial on the Fast Field Program (FFP) as applied to sound propagation in the air,'' Appl. Acoust. **27**, 203–215 (1989).

[17] S. J. Franke, C. Shaffer, R. Raspet, and C. H. Liu, ''Application of the Fast Field Program to blast noise prediction,'' Proc. 3rd Intl. Symp. Long Range Sound Propagation and Coupling Into the Ground, University of Mississippi, 28–30 March (1988), pp. 243–260.

[18] L. Attenborough, ''Acoustical impedance models for outdoor ground surfaces,'' J. Sound. Vib. **99**, 521–544 (1985).

[19] N. S. Yeowart and M. J. Evans, ''Thresholds of audibility for very low-frequency pure tones,'' J. Acoust. Soc. Am. **55**, 814–818 (1974).

[20] R. Heffner and H. Heffner, ''Hearing in the elephant (*Elephas maximus*),'' J. Comp. Physiol. Psychol. **96**, 926–944 (1982).

[21] A. D. Pierce, *Acoustics: An Introduction to Its Physical Principles and Applications* (McGraw-Hill, New York, 1981).

[22] W. R. Langbauer, R. Charif, R. Martin, K. Payne, and L. Osborn, ''Long-range monitoring of elephant movements and vocalizations'' (in preparation).